

# Increasing the regenerative braking energy for railway vehicles

Shaofeng Lu, Paul Weston, Stuart Hillmansen, Hoay Beng Gooi, and Clive Roberts

**Abstract**—Regenerative braking improves the energy efficiency of railway transportation by converting the kinetic energy into the electric energy. This paper proposes a method to apply the Bellman-Ford algorithm to search for the train braking speed trajectory to increase the total regenerative braking energy (RBE) in a blended braking mode with both electric and mechanical braking forces available. The Bellman-Ford (BF) algorithm is applied in a discretized train-state model. A typical suburban train has been modeled and studied under real engineering scenarios involving changing gradients, journey time and speed limits. It is found that the searched braking speed trajectory is able to achieve a significant increase on the RBE in comparison with the constant-braking-rate (CBR) method with only a minor difference on the total braking time. A RBE increment rate of 17.23% has been achieved. Verification of the proposed method using BF has been performed in a simplified scenario with zero gradient and without considering the constraints of braking time and speed limits. Linear Programming (LP) is applied to search for a train trajectory with the maximum RBE and achieves solutions that can be used to verify the proposed method using BF. It is found that it is possible to achieve a near-optimal solution using BF and the solution can be further improved with a more complex search space. The proposed method takes advantage on robustness and simplicity of modeling in a complex engineering scenario where a number of non-linear constraints are involved.

**Index Terms**—energy saving strategy, train braking energy increment, Bellman-Ford algorithm, dynamic programming, computation efficiency improvement

## I. INTRODUCTION

Energy conservation is becoming more important for modern rail transportation. It is reported that the traction energy accounts for 60%-70% of the total energy consumption in rail transport systems [1]. The traction energy is consumed to overcome the resistances and transformed into kinetic energy and heat energy. Regenerative braking converts the kinetic energy into electrical energy and thus reduces the total energy cost [2], [3].

A typical electric machine generally holds two working modes: motoring and regenerative mode. During motoring mode, the direction of motor rotating speed agrees with the direction of torque. On the contrary, when the direction of rotating speed opposes the direction of torque, electric machine enters the regenerative mode. For a railway vehicle, during the regenerative braking mode, the torque reduces the motor speed and generates the electric power.

The regenerative braking energy will be converted by power electronic devices into electric energy which can be fed back into the electric power grid in the AC electric network, and used by other adjacent running trains through the DC electric

network or stored in the energy storage devices (ESDs). Otherwise, the regenerative energy can be converted into heat using a large resistance bank referred to as the “dynamic braking” [4].

Regenerative braking takes a key role in energy efficiency for the rail transport. It is affected by various parameters and the parameters in a DC railway case are summarized in [5]. In order to improve energy efficiency via recapturing more regenerative braking energy, different methods have been adopted in past research.

- The integration of ESDs reduces the dependence on the power transmission network and increases the effective regenerative braking energy to be stored. Research work proposed in various research papers have focused on optimizing the ESDs to improve the energy efficiency [6]–[10].
- More regenerative energy can also be achieved by improving the receptivity of the DC network as the amount of recaptured regenerative energy is constrained by the network receptivity [11]. Timetable optimization, as one of the feasible methods, has been applied to improve the network receptivity to increase the recaptured regenerative braking energy [12].
- Optimization of the braking effort control strategy can lead to an improvement of energy efficiency. Optimization on the braking force distribution strategy is reported in [13], [14] to maximize the regenerative braking energy. The research work proposed by [15], [16] is focused on optimizing the braking torque based on the electric motor characteristics.

The optimization methods of the braking effort control can be achieved by the train speed trajectory optimization to some extent since the train speed trajectory is the direct consequence of the applied torque of the motor. A recent paper has considered the regenerative braking energy in their automatic train operation (ATO) speed profile design [17]. Optimal train control to locate the energy-efficient train speed trajectory has been extensively studied over the past two decades [18]–[21]. Regenerative braking in these studies can be involved as part of the constraints for the train control. The braking rate has also been taken into account for the speed profile optimization of a train with regenerative braking [22]. These papers only take the RBE as a part of the optimization objectives or constraints. The research work proposed in this paper, on the other hand, is focused on increasing the regenerative electric braking energy (RBE) via improving the train braking speed trajectory, referred to as the “braking trajectory”. While the maximization

of RBE does not necessarily lead to the maximization of the total journey energy efficiency, this paper is motivated by the energy efficiency improvement to be made by the braking trajectory optimisation. The research work proposed in the paper can be applied to evaluate the positive impact the regenerative braking may have on an existing railway route with limited spaces for an optimization of the entire speed trajectory, for example, a train required to operate aggressively. A suburban train has been modeled and the method of the modeling has been used in a number of previous works [23], [24]. It is assumed that the blended braking is applied where both electric and mechanical braking are available. A graphical search method, the Bellman-Ford (BF) algorithm [25], [26], is proposed to search for the optimal braking trajectory with the maximum RBE within the search space. The searched braking trajectory will be compared with the one using the constant braking rate to investigate the advantage of the proposed method. The proposed method will be further verified by the results achieved by Linear Programming (LP) in a simplified scenario.

The organization of this paper is as follows. Section I covers the background introduction, literature review and research motivation. Section II covers the formulation of the objective function and its optimization system modeling. Section III introduces the optimization method: the Bellman-Ford (BF) algorithm. Section IV demonstrates case studies for a suburban train using BF. Section V covers the verification of our proposed method. Finally, the conclusions are drawn in Section VI.

## II. SYSTEM MODELING

The braking process of a typical rail vehicle is modeled in a discrete manner shown in Fig. 1. To simplify the problem, it is assumed that the conversion from the kinetic energy to the electric energy is 100%. In Fig. 1, the braking candidate distance and speed are constrained by the forward and backward calculation using the maximum braking rate. Each train state is a combination of three variables: instant train speed  $v$  and braking time  $t$  and instant distance  $d$  from the final state shown in black circle in Fig. 1. Each grey round circle in Fig. 1 represents a group of train states with the same braking speed and distance but different braking time. Other train state should not have a zero speed or a speed exceeding the speed limit. The braking time for each train state since the final train state should not exceed the allowed braking time. If a train state is able to switch to another, the braking rate between these two states should be less than the maximum braking rate. In this paper, the train is allowed to keep its speed when it switches from one state to another, resulting a maximum acceleration rate of  $0 \text{ m/s}^2$ . If needed, the train can be allowed to re-motor and increase its speed in the braking process.

The modeling and optimization procedure is divided into the following three steps.

**Step 1** Determine the braking candidate distance and speed. The braking process is divided into different subdivisions between the starting position and the ending position. The position to divide the total braking distance is referred to

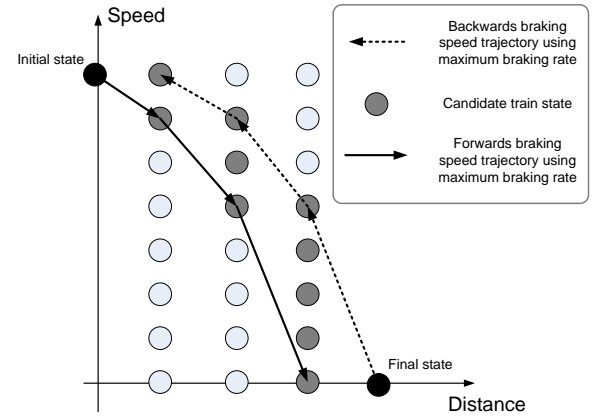


Fig. 1. The braking candidate distance and speed.

as the candidate position and the speed on each candidate position is referred to as the candidate speed. The speed at each candidate position is constrained between the two braking speed trajectories by backward and forward calculations using the maximum braking rate. Both calculations should not exceed the speed limit, if any, and lower than zero speed.

**Step 2** Generate the train states. The braking trajectory consists of a series of train state switches and is generated using the following Lomonosoff's equation in 1. A detailed introduction on the state-switch calculations has been covered in [23], [27].

$$M' \frac{dv}{dt} = F - (A + Bv + Cv^2) - Mg \sin(\alpha) \quad (1)$$

where,

- $F$  is the tractive effort or braking effort if applicable within the maximum acceleration and deceleration rate;
- $A$ ,  $B$  and  $C$  are the Davis coefficients;
- $M'$  is the effective mass including rotary allowance;
- $M$  is the tare mass;
- $g$  is the acceleration due to gravity;
- $v$  is the instantaneous train speed;
- $t$  is the instantaneous time; and
- $\alpha$  is the slope angle.

Between two train states with different speeds  $v_1$  and  $v_2$  and distances  $d_1$  and  $d_2$ , where  $v_2 > v_1$  and  $d_2 > d_1$ , the braking rate  $a_{br}$  is assumed to be constant and can be calculated in (2).

$$a_{br} = \frac{v_2^2 - v_1^2}{2(d_2 - d_1)} \quad (2)$$

The calculation of the total electric braking energy between every two train states will be further achieved in each minor iterative step. In each minor step, the total braking effort  $F_{tb}$  is calculated using the braking rate  $a_{br}$  obtained in (2). Assume that a train is with a speed at a minor distance of  $\Delta D$ . The total braking effort  $F_{tb}$  is a combination of the electrical braking force  $F_{eb}$  and the mechanical braking force  $F_{mb}$ . The electrical braking regenerative energy  $E_{eb}$  in each minor step is calculated in (3).

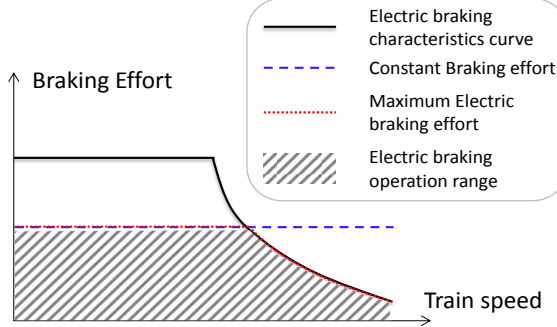


Fig. 2. Schematic diagram of various braking efforts.

$$E_{eb} = F_{eb} \Delta D \quad (3)$$

Assume that  $F_{eb}^{max}$  is the maximum available electrical braking force at current speed  $v$ . The electric braking force is represented by (4) and the total braking force is represented by (5).

$$F_{eb} = \min(F_{eb}^{max}, F_{tb}) \quad (4)$$

$$F_{tb} = a_{br} * M' \quad (5)$$

In Fig. 2, a schematic diagram of braking efforts is shown. The black solid line represents the maximum electric braking effort; the blue dashed line stands for an instantaneous constant braking effort imposed on the train during braking, the red dotted line represents the maximum feasible electric braking effort  $F_{eb}$  and the gray patterned area indicates the electric braking operation range.

**Step 3** Construct a directed weighted graph  $G = (V, E)$  for a shortest-path optimization. Using the method in the second step, one is able to calculate the RBE and time usage while a train is braking from one train state to another using the method in **Step 2**. In a graph  $G = (V, E)$ ,  $V$  is the set of vertices in a graph to represent the train speed state and  $E$  is to represent the set of edges connection between the states. The value for the RBE for braking between two states is negative. Thus, the shortest path of series of edges with minimum value between two states will represent the braking trajectory in association with the maximum RBE. The detail of the shortest path search algorithm will be covered in the next section. It is worth mentioning that journey time constraint will be imposed so that only the path within the demanded journey time window will be regarded as valid.

### III. THE BELLMAN-FORD ALGORITHM

The Bellman-Ford (BF) algorithm is commonly applied to compute single source shortest paths in a weighted directed graph [25], [26], [28]. Compared with Dijkstra's algorithm [29], BF is able to cope with graphs with negative edge weights. The worst case performance for BF is  $O(|V| * |E|)$  where  $|V|$  and  $|E|$  are the numbers of vertices and edges. Each vertex represents a train state and the distance between two

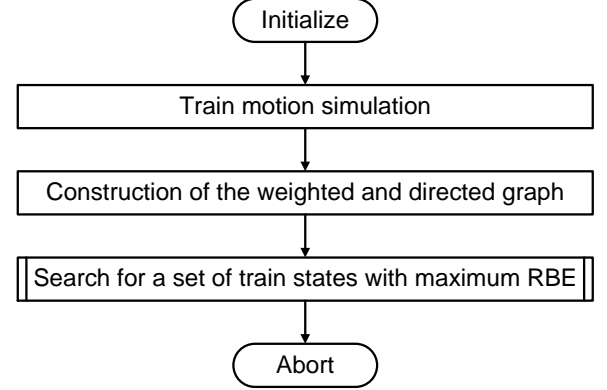


Fig. 3. Flow chart diagram for the proposed method using the Bellman-Ford algorithm.

vertices represents the RBE generated when the train switches from one state to another.

Before the illustration of BF, some definitions are made as follows:

- Let  $i$  and  $j$  be any vertices in the vertex set  $V$ :  $i, j \in V$ ;
- Let  $d[i]$  represent the shortest distance from the source for vertex  $i$  and it is set infinity for initialization;
- Let  $p[i]$  be the previous vertex for  $d[i]$ ;  $p[i] = \emptyset$  for the source vertex;
- Let  $w$  be the weight matrix where  $w(i, j)$  is the edge for vertices  $i$  and  $j$  representing the electric braking energy for trains states switching from vertex  $i$  to  $j$ .

For any vertex  $i$ , if there exists another random vertex  $j$ , through which  $i$  is able to achieve a shorter distance to the initial vertex than its current shortest path, the shortest path between  $j$  and the initial vertex will be replaced by the new path involving  $i$ . This is referred to a relaxation process and the **RELAX** function is used to perform this process. Note that the **RELAX** function will be repeated for each vertex to ensure that the distance for each vertex will be reduced to the minimum as long as there are no negative cycles. Negative cycles are eliminated by only allowing one-direction generation of train braking states at **Step 3**.

The pseudo-code for the **BELLMAN-FORD** and **RELAX** function is shown as follows. It is well known that BF

#### Algorithm 1 RELAX function

```

if  $w(i, j) + d[i] < d[j]$  then
     $d[j] \leftarrow w(i, j) + d[i]$ 
     $p[j] \leftarrow i$ 
end if

```

can become computationally infeasible if the search space grows large. In this paper, the following strategies are adopted to improve the computational efficiency. But nevertheless, a tradeoff between the optimality and computation efficiency should be maintained based on the system requirement.

- Parallel computation has been applied during the states generation. For example, the information of the travelling

**Algorithm 2 BELLMAN-FORD** function

```

for all  $i$  in  $V$  do ▷ Initialisation
     $d[i] \leftarrow \infty$  ▷ Original distance from each vertex to the
    source is infinity
     $p[i] \leftarrow i$  ▷ Previous vertex being itself
end for
for  $k := 1 \rightarrow (|V| - 1)$  do
    for all  $(i, j)$  in  $E$  do
         $RELAX(i, j, w, d, p)$ 
    end for
end for
for all  $(i, j)$  in  $E$  do ▷ Identify the negative cycle in the
graph
    if  $w(i, j) + d[i] < d[j]$  then
         $Return(FALSE)$ 
    else
        ...
    end if
end for

```

time and RBE between two train states can be obtained in parallel.

- Heuristics can be applied to eliminate two identical states. For example, if two train states with the same travelling time from the initial state, and the same current speed and distance, the one with the less RBE can be eliminated.
- The discretization of the state space can be applied. For example, as the journey time difference in second is insignificant, each states can be modeled with the unit second.

#### IV. CASE STUDIES

Case studies for a typical suburban train under a practical engineering scenario have been conducted. A suburban train will brake from a nominal speed until it finally stops. The total braking distance remains 1750 m in this paper. In addition to BF, the constant-braking-rate (CBR) method will also be applied. A random constant braking rate of  $0.5632 \text{ m/s}^2$  is proposed based on  $a = 0.5 * v^2/s$ , where  $v$  is the maximum train speed  $44.4 \text{ m/s}$  and  $s$  is the braking distance 1750 m. Actually, the constant braking rate can be varied to generate different braking curves within the braking distance. CBR is implemented in a backward calculation using this constant braking rate across the entire braking distance. The train will take a cruising operation when a speed limit is imposed. The initial speed and total braking time will then be determined by CBR and will also be used for BF. Using this backward calculation, the initial speed and proposed journey time for both methods obtained as  $41.8 \text{ m/s}$  and  $80.86 \text{ s}$  respectively. Note that other constraints such as the speed limits and gradients are imposed as well. Finally, the results achieved by CBR will be compared to the ones achieved by BF.

Fig. 4 shows the braking effort and resistance effort characteristics for a typical suburban train [30]. The Davis equation [31] is considered to account for the resistive force imposed on the train. The relative altitude profile is shown in Fig. 5.

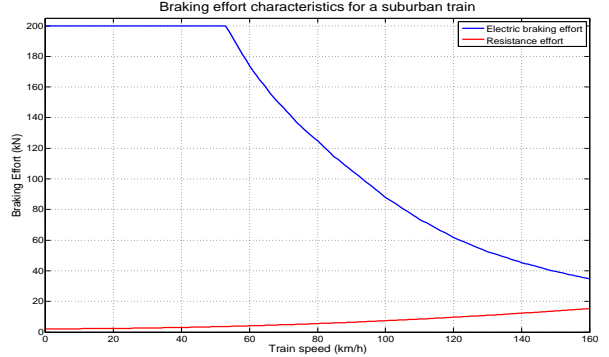


Fig. 4. Braking effort characteristics for a typical suburban train.

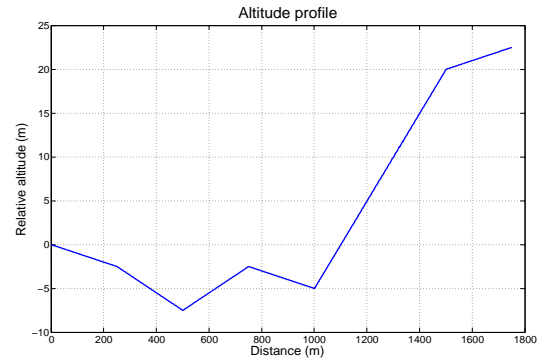


Fig. 5. Altitude profile for case 1.

TABLE I  
TRAIN VEHICLE MODELING PARAMETERS

$M(t)$	$M'(t)$	$P_{max}(\text{kW})$	$v_{max}(\text{km/h})$	$a_{br}^{max} (\text{ms}^{-2})$
170	178	3,681	160	1.2

All other essential parameters are listed in Tables I and II. Note that  $M$  and  $M'$  are the train mass and train effective mass in tonnes respectively.  $P_{max}$  is the maximum train generation power.  $v_{max}$  is the maximum allowed train speed.  $a_{br}^{max}$  is the maximum train braking rate. In Table II, the minimum distance interval is the minimum distance between two train states. The maximum distance interval will be adopted to ensure that the gradients and speed limits remain the same within one distance interval. The minor distance interval is the iterative simulation step to calculate the energy consumption between two train states. The minimum speed interval and the time interval are the minimum difference between the speed and time of every two states with two of the elements being the same. For example, if both the distance and speed are the same for two train states, the time difference between them should not be less than the minimum time interval.

After the electric braking energy is calculated using the single train simulator, a weighted connected graph will be created and the implementation of BF is applied using the MatlabSGL library in MATLAB [32].

The total RBE achieved by CBR and BF are denoted by

TABLE II  
GRAPH MODELING PARAMETERS

Minimum distance interval (m)	100
Maximum distance interval (m)	200
Minor distance interval(m)	1
Minimum speed interval (m/s)	0.1
Minimum time interval (s)	1

TABLE III  
SIMULATION RESULTS

$T_{CBR}$ (s)	$T_{BF}$ (s)	$E_{CBR}^{eb}$ (kWh)	$E_{BF}^{eb}$ (kWh)	Increment Rate(%)
80.86	82.48	27.46	32.19	17.23

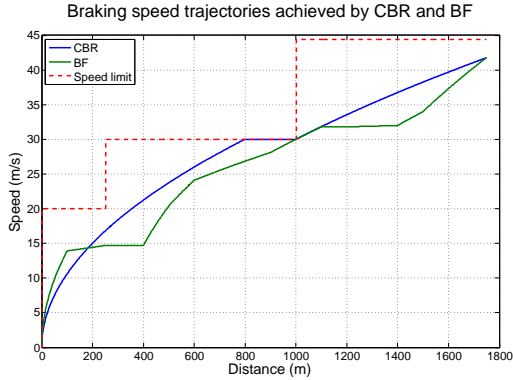


Fig. 6. Comparison of the braking speed trajectories by CBR and BF.

$E_{CBR}^{eb}$  and  $E_{BF}^{eb}$  respectively. The total braking time by these two methods are denoted by  $T_{CBR}$  and  $T_{BF}$ . BF searches a braking speed trajectory with various braking rates so that the RBE can be maximized within the search space.

Table III summarizes the simulation results. A comparison of the braking speed trajectories achieved by CBR and BF is shown in Fig. 6. The electric braking effort (EBE) and total braking effort (TBE) by both methods are demonstrated in Fig. 7. In Fig. 7, the EBE in solid lines and the TBE in dashed lines are shown for both braking trajectories achieved by BF and CBR.

In Table III, it is found that using BF, an increase of RBE can be significantly achieved compared to the one by CBR. A slight deviation on the journey time for BF can be observed. In Fig. 7, the EBE in solid lines and the TBE in dashed lines are shown for both braking trajectories achieved by BF and CBR.

It has been demonstrated that BF takes advantage by incorporating the nonlinear constraints into the states generation and is able to solve the RBE-maximization problem in a relatively convenient way. As will be demonstrated in Section V, the state discretization prevents BF from obtaining a globally optimal solution but an increase of train states can be realized by reducing the minimum distance between every two train states and will lead to an increase of the achieved maximum RBE and a longer computation time.

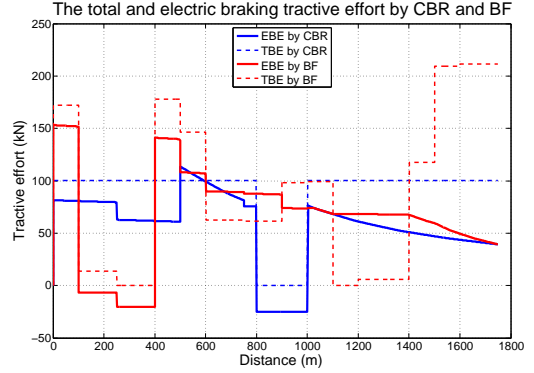


Fig. 7. Comparison of the braking effort by CBR and BF.

## V. VERIFICATION OF THE PROPOSED METHOD

In this section a simplified case scenario where a train is braking on a level track with only non-positive braking forces applied will be discussed. With a reasonable approximation, Linear Programming (LP) can achieve an optimal braking trajectory with the maximum RBE. The results achieved by LP will be used to verify our proposed method. A RBE-maximization model is proposed and solved by LP. The details of the modeling are covered in V-A.

### A. Linear programming modeling

As shown in Appendix A, it can be proved that if the initial train speed is either too high or too low, an optimal solution for the RBE-maximization problem in a simplified scenario will only include part or all of the following three operations:

- maximum-braking operation;
- maximum-electric-braking operation;
- coasting operation.

Since the resistance exists along the entire braking operation, the optimal train braking speed trajectory will keep decreasing until a full stop. Assume that  $v_1, v_2, \dots, v_N$  are a set of speeds on the reducing braking speed trajectory of a train with  $v_N$  being zero and  $v_1$  being the initial speed before braking.  $N$  is a sufficiently large number and represents for the total number of the intermittent candidate speeds.  $N$  is large enough to ensure the speed change between two adjacent candidate speeds is so small that the average speed calculated based on these two speeds will be able to closely approximate the actual average speed with a satisfactory precision. A schematic diagram for the discretized braking speed versus distance is shown in Fig. 8.

It is assumed that the difference between two adjacent braking speeds is constant. Therefore, as long as the initial and the final speed are known, all the intermittent speeds  $v_i$   $i = 2, 3, \dots, N - 1$  will be known and can be calculated using (6).

$$v_i = v_1 - (i - 1) \frac{v_N - v_1}{N - 1} \quad i = 2, 3, \dots, N - 1 \quad (6)$$

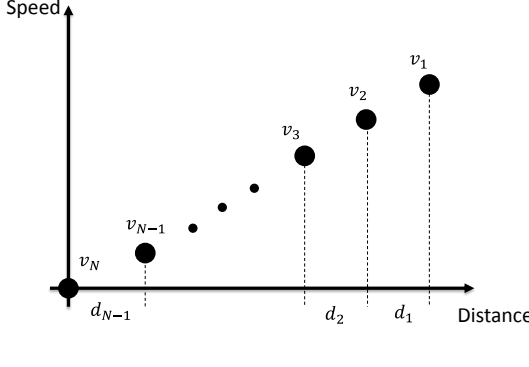


Fig. 8. Braking speeds vs. distance in for the LP application.

The average speed  $v_i^a$  between  $v_i$  and  $v_{i+1}$  is calculated by (7).

$$v_i^a = (v_i + v_{i+1})/2 \quad i = 1, 2, \dots, N - 1 \quad (7)$$

The average resistance between  $v_i$  and  $v_{i+1}$  is calculated by (8).

$$F_i^{re} = A + Bv_i^a + C(v_i^a)^2 \quad i = 1, 2, \dots, N - 1 \quad (8)$$

where, A, B and C are the Davis coefficients.

The average maximum electric braking effort between  $v_i$  and  $v_{i+1}$ , denoted by  $F_i^{e,max}$  can be obtained by linearly incorporating the braking characteristics shown in Fig. 4 using  $v_i^a$ .

The distance between  $v_i$  and  $v_{i+1}$  is denoted by  $d_i$ ,  $i = 1, 2, 3, \dots, N - 1$ . The total distance constraints should be met as defined in (9).

$$D = \sum_{i=1}^{N-1} d_i \quad (9)$$

where  $D$  is the total braking distance.

The average deceleration rate will be defined as:

$$a_i^{br} = \frac{v_{i+1}^2 - v_i^2}{2d_i} \quad (10)$$

$a_i^{br}$  should be less than the maximum braking rate  $a_{br}^{max}$  as shown in Table I. Hence, (11) can be derived.

$$\frac{v_{i+1}^2 - v_i^2}{2d_i} \leq a_{br}^{max} \quad (11)$$

It consequently yields:

$$d_i \geq \frac{v_{i+1}^2 - v_i^2}{2a_{br}^{max}} \quad (12)$$

The RBE at  $d_i$ , denoted by  $E_i^{eb}$ , between  $v_i$  and  $v_{i+1}$  should meet the following two linear constraints.

$$\begin{aligned} E_i^{eb} &\leq (M' a_i^{br} - F_i^{re}) d_i \\ &\leq M' \frac{v_{i+1}^2 - v_i^2}{2} - (A + Bv_i^a + C(v_i^a)^2) d_i \end{aligned} \quad (13)$$

$$E_i^{eb} \leq F_i^{e,max} d_i \quad (14)$$

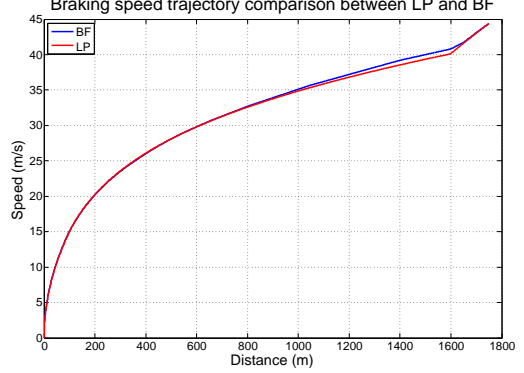


Fig. 9. Comparison of the speed trajectories achieved by BF and LP with an initial speed of 44.4 m/s.

TABLE IV  
RESULTS COMPARISON BETWEEN BF AND LP

	$E_{BF}^{eb}$ (kWh)	$E_{LP}^{eb}$ (kWh)
$v_1 = 35.0$ m/s	27.78	28.85
$v_1 = 44.4$ m/s	37.60	38.38

Both (13) and (14) ensure similar constraints set by (4). The electric braking effort should be less than the maximum electric braking effort and the braking effort defined by the total braking rate and average resistance.

LP is applied to solve the model defined by the above mentioned constraints. In this paper, IBM ILOG CPLEX [33] has been applied to solve this optimization model and the results will be shown and discussed in Section V-B.

#### B. Results and discussions

In this section, the optimization results achieved by LP and BF for a simplified scenario will be compared and discussed. In order to ensure that the results achieved by LP are close enough to the optimal solution, the difference between two adjacent candidate speeds is set as “0.1 m/s” and it is found that a further reduction of the difference does not further improve the result.

Two braking scenarios with initial braking speeds of 44.4 m/s and 35.0 m/s are proposed. Both LP and BF are applied to search for the braking trajectory with a maximum RBE in their search space. Fig. 9 and Fig. 10 demonstrate the optimization results with an initial braking speed of 44.4 m/s. Fig. 11 and Fig. 12 demonstrate the optimization results with an initial braking speed of 35.0 m/s.

Let  $E_{BF}^{eb}$  and  $E_{LP}^{eb}$  denote the RBE achieved by BF and LP respectively. Let  $v_1$  denote the initial speed. The results are summarised in Table IV. In Fig. 9 and Fig. 11, it is observed that BF is able to achieve a braking trajectory close to the one generated by LP. With regards to the braking effort, BF is only able to control the braking rate in a discretized manner producing a discrete braking effort profile. In Table IV, it is

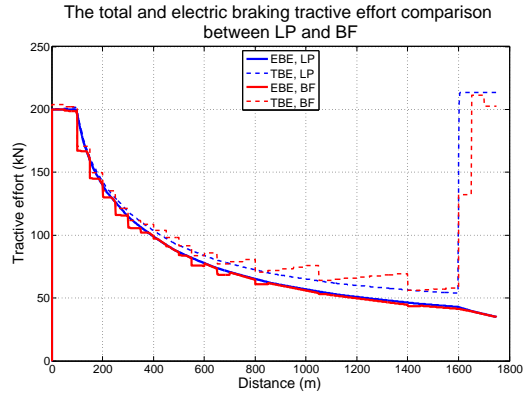


Fig. 10. Comparison of the braking efforts achieved by BF and LP with an initial speed of 44.4 m/s.

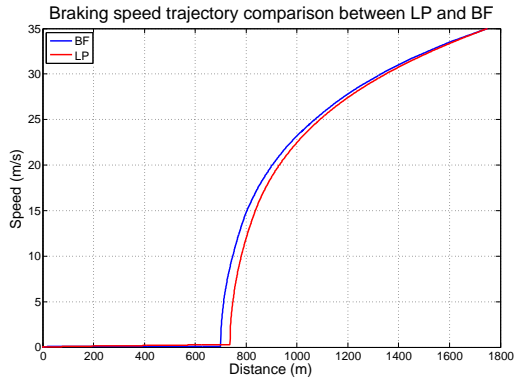


Fig. 11. Comparison of the speed trajectories achieved by BF and LP with an initial speed of 35.0 m/s.

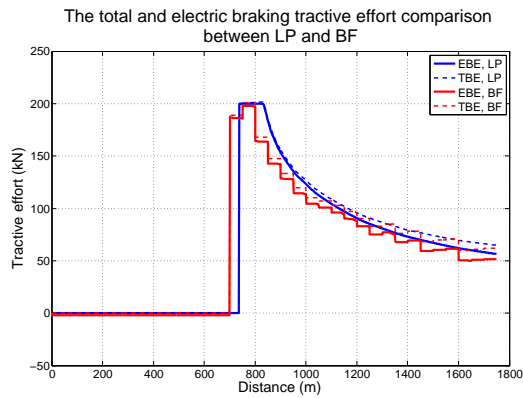


Fig. 12. Comparison of the braking efforts achieved by BF and LP with an initial speed of 35.0 m/s.

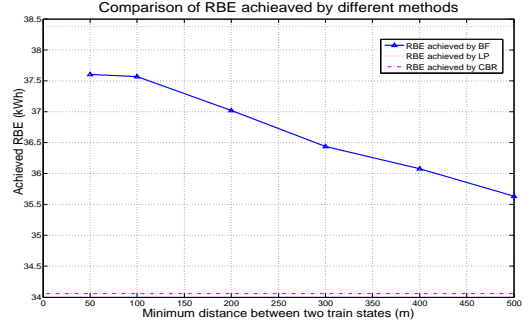


Fig. 13. Comparison of RBE achieved by BF, LP and CBR with an initial speed of 44.4 m/s.

noted that BF is unable to achieve a solution as good as the one achieved by LP due to discretization.

In this paper, the minimum distance between two train states has been varied to change the total generated train states. A shorter minimum distance leads to more train states being generated. Generally, more train states will lead to more RBE and the achieved solution will gradually approach a global optimal solution by searching all the possible train states. However, due to “the curse of dimensionality” the train states will increase so greatly that optimization by BF will be practically impossible due to the limited computation capability. A sensitivity analysis has been conducted between the RBE achieved and the minimum distance between two train states for the case with an initial speed of 44.4 m/s. For comparison reasons, the RBE achieved by both LP and CBR are also demonstrated. The constant braking rate can be simply obtained from the total braking distance and the initial braking speed. The results are shown in Fig. 13.

In Fig. 13, it is found that an increase of the minimum distance between every two train states will lead to less RBE. A minimum distance of 50 m between two train states will generate a total RBE of 37.60 kWh which is also shown in Table IV and a higher minimum distance will reduce the train states and RBE achieved. Compared to the results by CBR, it is noted that BF is able to achieve a significant increase on the RBE in this simplified case. It is observed that BF is only able to achieve a sub-optimal solution due to discretization of the train states, but a significant increase of RBE can be achieved compared to the one achieved by CBR with desirable simplicity and robustness. Note that LP cannot be applied in nonlinear cases, the advantages of BF becomes significant when a train is required to brake along a distance with various speed limits and gradients.

## VI. CONCLUSIONS

It is demonstrated in this paper that the RBE can be significantly increased for the searched train braking trajectory compared to the conventional braking trajectory using a nominal constant braking rate. A shortest path search method, i.e. the Bellman-Ford (BF) algorithm has been proposed to search for the braking trajectory to increase the RBE generated. BF has been applied in a case scenario with nonlinear constraints, such as speed limits, gradients and braking time constraints.

The optimization results demonstrate that a significant increase can be achieved compared to the one by a constant braking rate. The solutions by BF has also been verified by LP in a simplified case scenario. The obtained braking trajectory is suitable to provide a guidance during braking operation. Future works will be to develop an algorithm to improve the computation efficiency of the algorithm for the RBE optimization problem. Conclusions of this paper are drawn as follows:

- In a discretized train states space, BF is able to search for the optimal braking trajectory with the maximum RBE under different constraints with a high level of robustness. A good tradeoff between the computation efficiency and solution quality should be maintained.
- In a case scenario with speed limits, non-zero gradients and a narrow allowable braking time window, BF is able to locate a train braking trajectory with a significant increase in RBE compared to the one achieved by CBR.
- In a simplified case scenario, an optimal solution can be achieved by LP and has been used as verification for BF. The RBE achieved by BF is slightly less than the one by LP. However, an increase of RBE can be obtained compared to the one achieved by CBR. The proposed method using BF takes advantage on its easiness and robustness on the application in a case scenario with nonlinear constraints.

#### APPENDIX A OPTIMALITY ANALYSIS USING PONTRIYAGIN'S MAXIMUM PRINCIPLE

Similar to Section V, no speed limits and journey time constraints are considered for a train on a zero-gradient track in this section. Only braking force can be applied in mechanical or electrical braking. This implies that the speed of train will be at least decreased by resistance. An optimality analysis for a braking trajectory to achieve the maximum braking energy is conducted using the Pontryagin's Maximum Principle. Similar studies have been proposed for the optimisation of the entire train trajectory in papers [18]–[21]. The motion of train during braking is modeled by (15) and (16).

$$\frac{dt}{ds} = \frac{1}{v} \quad (15)$$

$$M'v \frac{dv}{ds} = f_{eb} + f_{mb} - f_r \quad (16)$$

where  $t$  is the time;  $s$  is the distance;  $v$  is the train speed during braking;  $f_{eb}$ ,  $f_{mb}$  and  $f_r$  are the electric braking force, mechanical braking force and resistance respectively. Since zero gradient is considered, the force due to the gravity is omitted.  $f_{eb}$  is the electric braking force between zero and the maximum negative braking force  $f_{eb}^{n-max}$  as it is assumed that no motoring is allowed during this simplified braking process with a speed which keeps decreasing by resistance and possible braking force.  $f_{eb}^{n-max}$  depends on the current speed.  $f_{mb}$  is a non-positive mechanical braking force limited by the maximum braking rate.  $M'$  is the train effective mass accounting for the rotary inertia.  $f_r$  is the force depending on

the current speed, specifically it can be presented by (17).

$$f_r(v) = A + Bv + Cv^2 \quad (17)$$

where  $A$ ,  $B$  and  $C$  are the Davis coefficients.

The instantaneous RBE  $E_{eb}$  recovered is represented by (18).

$$\frac{dE_{eb}}{ds} = -f_{eb} \quad (18)$$

where the braking operation with a negative  $f_{eb}$  increases the RBE.

Assume that the total braking distance is  $S$  with an initial speed of  $v_1$ . The boundary conditions are shown as (19).

$$\begin{aligned} t(0) &= 0 & t(S) &< \infty \\ v(0) &= v_1 & v(S) &= 0 \end{aligned} \quad (19)$$

Based on the Pontryagin's Maximum Principle (PMP), the Hamiltonian is defined as:

$$\begin{aligned} H &= \frac{dE_{eb}}{ds} + \lambda_1 \frac{dv}{ds} + \lambda_2 \frac{dt}{ds} \\ &= -f_{eb} + \frac{\lambda_1}{M'v} (f_{eb} + f_{mb} - f_r) + \frac{\lambda_2}{v} \\ &= \left( \frac{\lambda_1}{M'v} - 1 \right) f_{eb} + \frac{\lambda_1}{M'v} f_{mb} + \frac{\lambda_1}{M'v} (-f_r) + \frac{\lambda_2}{v} \end{aligned} \quad (20)$$

$f_{eb}$  and  $f_{mb}$  are the two control inputs. Let  $\mu$  denote the term  $\frac{\lambda_1}{M'v}$ . Based on PMP, in order to maximize the Hamiltonian, the following observations can be made.

- If  $\mu > 1$ , both  $f_{eb}$  and  $f_{mb}$  should be zero. This corresponds to a coasting operation.
- If  $\mu \in (0, 1)$ ,  $f_{eb}$  should be as negative as possible while  $f_{mb}$  should be zero.  $f_{eb} = f_{eb}^{n-max}$  if the resulted braking rate does not exceed the maximum braking rate. This operation is referred as the “full-electric-braking operation”.
- If  $\mu < 0$ , both  $f_{eb}$  and  $f_{mb}$  should be as negative as possible.  $f_{eb}$  should increase first. The maximum braking rate constraints should be met. This operation is referred as the “full-braking operation”.
- If  $\mu = 0$  or  $\mu = 1$ , a singular mode of train control will result.

Two adjoint equations are as follows.

$$\frac{d\lambda_1}{ds} = -\frac{\partial H}{\partial v} \quad (21)$$

$$\frac{d\lambda_2}{ds} = -\frac{\partial H}{\partial t} = 0 \quad (22)$$

$v$  is a variable which depends on  $s$  and together with (21), (15) and (16) we derive:

$$\frac{d\mu}{ds} = \frac{1}{M'v^3} (\lambda_2 + \mu v^2 f'_r(v)) \quad (23)$$

where  $f'_r(v)$  is the derivative of (17), namely  $f'_r(v) = B + 2Cv$ .

In a singular operation mode,  $\mu = 1$  or  $\mu = 0$ , so  $\frac{d\mu}{ds} = 0$ . Given that  $\lambda_2$  is constant based on (22), it can be derived that:

$$-V^2 f'_r(V) = \lambda_2 \quad (24)$$

where  $V$  is a constant speed during both singular modes.

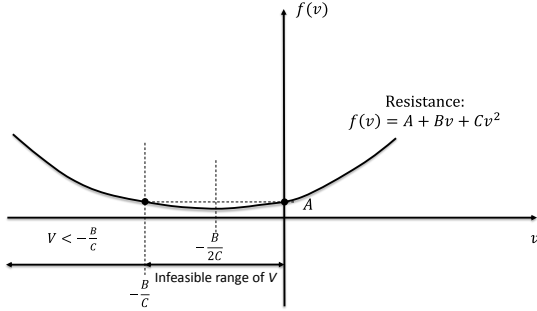


Fig. 14. The feasible range of the speed during a singular mode.

The non-zero resistance defined by (17) is always against the motion of train and only non-positive electric or mechanical braking forces can be imposed. In order to keep a constant speed, the speed should be less than zero, so that the negative braking force can be equal to the resistance but in an opposite direction. In addition,  $V$  cannot be between 0 and  $-\frac{B}{C}$  because the resistance cannot be less than  $A$ . It also means that the singular mode due to  $\mu = 0$  is infeasible. Within the proposed modeling context, if  $\mu = 0$ ,  $V = 0$  and the train is unable to keep a zero speed with a constant negative resistance  $A$  and non-positive braking force. Therefore,  $f'_r(V) < -B \leq 0$  for  $V < -\frac{B}{C}$ . A schematic diagram is shown in Fig. 14 for illustration of the feasible range of the speed during a singular mode due to  $\mu = 1$ .

A variable  $\xi$  is defined as follows.

$$\xi = \frac{-V^2 f'_r(V)}{v^2 f'_r(v)} \quad (25)$$

It is noted that  $\xi < 0$  since  $f'_r(V) < 0$  and  $f'_r(v) > 0$ . By rearranging ((23)) and it derives:

$$\begin{aligned} \frac{d\mu}{ds} &= \frac{1}{M'v^3} (\lambda_2 + \mu v^2 f'_r(v)) \\ &= v^2 f'_r(v) \frac{1}{M'v^3} (\mu + \frac{\lambda_2}{v^2 f'_r(v)}) \\ &= \frac{f'_r(v)}{vM'} (\mu - \xi) \end{aligned} \quad (26)$$

It is noted that  $\frac{f'_r(v)}{vM'} > 0$  given that  $v > 0$ ,  $f'_r(v) > 0$  and  $M' > 0$ . There are 4 possible cases with regard to the initial value of  $\mu$ .

**Case 1** If initially  $\mu \in (1, \infty)$ ,  $\mu > \xi$  and  $\frac{d\mu}{ds} > 0$ .  $\mu$  will keep increasing and the train will keep coasting until the end.

**Case 2** If initially  $\mu \in (0, 1)$ ,  $\mu > \xi$  and  $\frac{d\mu}{ds} > 0$ . As a result, the full-electric-braking operation should apply.  $\frac{d\mu}{ds} > 0$ ,  $\mu$  will keep increasing to be more than 1 and thus a coasting operation will be applied until the end.

**Case 3** If initially  $\mu \in (\xi, 0)$ ,  $\mu > \xi$  and the full-braking operation should be applied.  $\mu$  will also keep increasing and operations in **Case 2** and **Case 1** will apply subsequently.

**Case 4** If initially  $\mu \in (-\infty, \xi)$ ,  $\mu < \xi$  and the operations in **Case 3** will apply. However, in this case,  $\frac{d\mu}{ds} < 0$ ,  $\mu$  will keep decreasing and the full-braking operation always applies.

Hence, the train will keep braking with maximum braking force until the end.

It is noted that **Case 1** and **Case 4** cannot occur in most cases. Only coasting and full-braking operation will hardly achieve a desirable braking trajectory. Without considering the journey time and speed limits, the optimal braking control on a level track will be with an initial  $\mu \in (\xi, 0)$  or  $\mu \in (0, 1)$ . Therefore, an optimal braking operation involves the full-braking operation, the full-electric-braking operation and a coasting operation subsequently. These three operations may not necessarily co-exist but the operation order will remain the same i.e. a coasting operation comes after the full-electric-braking operation and the full-electric-braking operation comes after the full-braking operation. If a train has a very high initial speed and cannot brake using the full-braking operation, no feasible solution exists. Similarly, if a train has a very low speed and cannot maintain a positive speed before reaching the next station, no feasible solution exists as well. In such a case, motoring operations will be necessary to achieve a feasible braking trajectory.

## REFERENCES

- [1] P. Zhou and H. Xu, "Train coordinated optimization operation with regenerative braking," *Journal of Computers*, vol. 7, pp. 1025–1033, 2012.
- [2] A. Adinolfi, R. Lamedica, C. Modesto, A. Prudenzi, and S. Vimercati, "Experimental assessment of energy saving due to trains regenerative braking in an electrified subway line," *Power Delivery, IEEE Transactions on*, vol. 13, pp. 1536–1542, 1998.
- [3] S. Goh, M. Griffith, and K. Larbi, "Energy saving by using regenerating braking as normal train operation," in *4th. International Conference on Railway Traction Systems*, IET. IET, 2010.
- [4] Y. Sakamoto, T. Kashiwagi, M. Tanaka, H. Hasegawa, T. Sasakawa, and N. Fujii, "Rail brake system using a linear induction motor for dynamic braking," *Electrical Engineering in Japan*, vol. 179, pp. 29–38, 2012.
- [5] S. Acikbas and M. T. Soylemez, "Parameters affecting braking energy recuperation rate in dc rail transit," in *ASME Conference Proceedings*, 2007, pp. 263–268.
- [6] M. Ogasa, "Energy saving and environmental measures in railway technologies: Example with hybrid electric railway vehicles," *IEEJ Transactions on Electrical and Electronic Engineering*, vol. 3, pp. 15–20, 2008.
- [7] S. Hillmansen and C. Roberts, "Energy storage devices in hybrid railway vehicles: A kinematic analysis," *Proceedings of the Institution of Mechanical Engineers, Part F: Journal of Rail and Rapid Transit*, vol. 221, pp. 135–143, 2007.
- [8] F. Foiadelli, M. Roscia, and D. Zaninelli, "Optimization of storage devices for regenerative braking energy in subway systems," in *Power Engineering Society General Meeting, 2006. IEEE*, 2006.
- [9] J. Dixon and M. Ortuzar, "Ultracapacitors + dc-dc converters in regenerative braking system," *Aerospace and Electronic Systems Magazine, IEEE*, vol. 17, no. 8, pp. 16 – 21, Aug. 2002.
- [10] D. Iannuzzi, "Improvement of the energy recovery of traction electrical drives using supercapacitors," in *Power Electronics and Motion Control Conference*, 2008, pp. 1469–1474.
- [11] J. B. Forsythe, "Light rail/rapid transit: New approaches for the evaluation of energy savings, part ii - on the receptivity of a transit system," *Industry Applications, IEEE Transactions on*, vol. IA-16, no. 5, pp. 665 –678, Sep. 1980.
- [12] A. Nasri, M. Moghadam, and H. Mokhtari, "Timetable optimization for maximum usage of regenerative energy of braking in electrical railway systems," in *Power Electronics Electrical Drives Automation and Motion (SPEEDAM), 2010 International Symposium on*, Jun. 2010, pp. 1218 – 1221.
- [13] J. Zhang, B. Song, and X. Niu, "Optimization of parallel regenerative braking control strategy," in *Vehicle Power and Propulsion Conference, 2008. VPPC '08. IEEE*, Sep. 2008, pp. 1–4.
- [14] J. Guo, J. Wang, and B. Cao, "Study on braking force distribution of electric vehicles," in *Power and Energy Engineering Conference, 2009. APPEEC 2009. Asia-Pacific*, Mar. 2009, pp. 1–4.

- [15] L. Chu, F. Zhou, J. Guo, and M. Shang, "Investigation of determining of regenerative braking torque based on associated efficiency optimization of electric motor and power battery using ga," in *Electronic and Mechanical Engineering and Information Technology (EMEIT), 2011 International Conference on*, vol. 6, Aug. 2011, pp. 3238–3241.
- [16] Y. Wang, J. Miao, and Y. Wei, "The research of traction motor energy-saving regenerative braking control technology," in *Intelligent Computation Technology and Automation (ICICTA), 2010 International Conference on*, vol. 3, May 2010, pp. 930–933.
- [17] M. Domínguez, A. Fernández-Cardador, A. P. Cucala, and R. R. Pecharromán, "Energy savings in metropolitan railway substations through regenerative energy recovery and optimal design of ato speed profiles," *Automation Science and Engineering, IEEE Transactions on*, vol. 9, no. 3, pp. 496–504, Jul. 2012.
- [18] P. G. Howlett, P. J. Pudney, and X. Vu, "Local energy minimization in optimal train control," *Automatica*, vol. 45, no. 11, pp. 2692–2698, 2009.
- [19] P. Howlett, "The optimal control of a train," *Annals of Operations Research*, vol. 98, pp. 65–87, 2000.
- [20] E. Khmelnitsky, "On an optimal control problem of train operation," *IEEE transactions on automatic control*, vol. 45, no. 7, pp. 1257–66, 2000.
- [21] R. Liu and I. M. Golovitcher, "Energy-efficient operation of rail vehicles," *Transportation Research Part A: Policy and Practice*, vol. 37, no. 10, pp. 917–932, 2003.
- [22] Y. Bocharnikov, A. Tobias, C. Roberts, S. Hillmansen, and C. Goodman, "Optimal driving strategy for traction energy saving on dc suburban railways," *Electric Power Applications, IET*, vol. 1, no. 5, pp. 675–682, Sep. 2007.
- [23] S. Lu, S. Hillmansen, and C. Roberts, "A power-management strategy for multiple-unit railroad vehicles," *Vehicular Technology, IEEE Transactions on*, vol. 60, pp. 406–420, 2011.
- [24] N. Zhao, C. Roberts, and S. Hillmansen, "The application of an enhanced brute force algorithm to minimise energy costs and train delays for differing railway train control systems," *Proceedings of the Institution of Mechanical Engineers, Part F: Journal of Rail and Rapid Transit*, 2012. [Online]. Available: <http://pif.sagepub.com/content/early/2012/11/28/0954409712468231.abstract>
- [25] R. Bellman, "On a routing problem," *Quarterly of Applied Mathematics*, pp. 87–90, 1958.
- [26] J. L. R. Ford, D. R. Fulkerson, and R. G. Bland, *Flows in Networks*. Princeton University Press, 2010.
- [27] S. Lu, S. Hillmansen, T. K. Ho, and C. Roberts, "Single-train trajectory optimization," *Intelligent Transportation Systems, IEEE Transactions on*, vol. PP, no. 99, pp. 1–8, 2013.
- [28] T. H. Cormen, C. E. Leiserson, R. L. Rivest, and C. Stein, *Introduction to algorithms*, 3rd ed. Massachusetts Institute of Technology Press, 2009.
- [29] E. W. Dijkstra, "A note on two problems in connexion with graphs," *Numerische Mathematik*, vol. 1, pp. 269–271, 1959.
- [30] J. Johnson, "T860: Benefits of all electric braking," Rail Safety and Standards Board, Tech. Rep., 2011.
- [31] B. P. Rochard and F. Schmid, "A review of methods to measure and calculate train resistances," *Proceedings of the Institution of Mechanical Engineers, Part F: Journal of Rail and Rapid Transit*, vol. 214, pp. 185–199, 2000.
- [32] D. Gleich, "Matlabbgl library," Matlab central, 2008.
- [33] IBM, *IBM ILOG CPLEX V12.1- User's Manual for CPLEX*, 2009.



**Paul Weston** B.Eng (Electronics and Control Engineering, Birmingham, 1992), PhD (Nonlinear System Identification, Birmingham, 1999) has worked in the railway research group of the University of Birmingham as a Research Fellow since 2002 on electronics hardware, firmware, software and signal processing algorithms. Current research interests include railway vehicle energy instrumentation and modeling; railway asset condition monitoring instrumentation and signal processing.



**Stuart Hillmansen** is a Senior Lecturer in Electrical Energy Systems within the school of Electronic, Electrical and Computer Engineering at the University of Birmingham. He completed a PhD in Imperial College London. His main area of research interest is in hybrid traction systems for use in railway vehicles, and modeling and measurement of energy consumption for railway systems (both AC and DC). He is a member of the Birmingham Centre for Railway Research and Education. He leads the Railway Traction Research Group whose portfolio of activities is supported by the railway industry and government. He has authored a number of papers on railway energy consumption and presented the work at a number of international conferences. He is on the editorial board of the Proceedings of the Institution of Mechanical Engineers, Part F: Journal of Rail and Rapid Transit.



**Hoay Beng Gooi** received the B.S. degree from National Taiwan University in 1978, M.Sc. degree from the University of New Brunswick, Fredericton, NB, Canada, in 1980, and the Ph.D. degree from Ohio State University, Columbus, in 1983. From 1983 to 1985, he was an assistant professor in the EE Department at Lafayette College, Caston, PA. From 1985 to 1991, he was a senior engineer with Empros (now Siemens), Minneapolis, MN, where he was responsible for the design and testing coordination of domestic and international energy management system (EMS) projects. In 1991, he joined the school of electrical and electronic engineering, Nanyang Technological University (NTU), Singapore, as a Senior Lecturer. Since 1999, he has been an associate professor at NTU. His current research focuses on microgrid energy management systems, electricity markets, spinning reserve, energy efficiency, and renewable energy sources.



**Clive Roberts** is Professor in Railway Systems and Director at the University of Birmingham's Centre for Railway Research and Education. His PhD focussed on Condition Monitoring of Railway Infrastructure. Over the last 14 years he has developed a portfolio of research in the fields of railway systems engineering; system modeling and simulation; network capacity research; railway fault detection and diagnosis; and data collection and decision support applied to railway traction, signalling, mechanical interactions and capacity. He currently leads a team of 11 research fellows and 16 PhD students.



**Shaofeng Lu** is a Lecturer with Department of Electronic and Electrical Engineering, Xi'an Jiaotong-Liverpool University, China. He received the BEng and PhD degree from the University of Birmingham in 2007 and 2011 respectively. He also has a BEng degree from Huazhong University of Science and Technology, Wuhan, China. All are in Electrical and Electronic Engineering. His main research interests include power management strategies, railway traction system modeling, optimization techniques application and energy-efficient transportation systems.